ATMOSPHERIC CONDENSATION POTENTIAL OF WINDOWS IN HOT, HUMID CLIMATES

R. El Diasty
School of Architecture,
Arizona State University,
Tempe, AZ 85287-1605

I. Budaiwi
Centre for Building Studies,
Concordia University, Montréal,
Québéc, H3G -1M8, Canada.

ABSTRACT

In hot, humid climates, the internal surfaces of windows in air-conditioned buildings are in contact with relatively colder air. Meanwhile, the external surfaces are exposed to hot humid atmospheric air. This hygro-thermal condition may cause frequent atmospheric condensation on external surfaces of windows when their surface temperature drops below the dew point temperature of the hot humid air. To date, external surface condensation on windows has been given relatively much less importance than their internal surface condensation. In addition, the thermal analysis of windows in hot humid climates has always been performed in the absence of condensation. Under moderate air temperature and humidity conditions, such practice is acceptable. However, when windows experience atmospheric condensation on their external surfaces, the effect of condensation on window energy loss needs to be examined. In this paper, the external condensation process is analyzed and the atmospheric water vapor mass condensation rate has been obtained by utilizing a simplified transient uni-dimensional finite difference model. The results show that this model has enhanced the assessment of the potential for atmospheric condensation on windows in hot, humid climates and in predicting the amount of condensation expected, as well as the associated energy loss for given thermal and moisture conditions. The numerical computation of the model is able to account for condensation and its impact on the temperature gradient across the window. Thermal analysis of both single and insulated double-glazed windows under condensation conditions is presented. The work also includes the computational procedure used and the results of a case study demonstrating the model's capabilities.

INTRODUCTION

The quality of the building environment is known to be influenced by the presence of windows, particularly under climate extremes that impose limitation on outdoor activities. Since high temperature and humidity are characteristics of hot, humid climates, windows gain more importance as more time is spent indoors in the air-conditioned comfort, away from the heat and the undesirably high humidity. The visual linkage with the outside world and the admission of daylight and sunlight are among psychological and physiological function of the windows, that are affected particularly when surface condensation is present for long periods of time. Distorted and obscured vision through windows is common when condensation takes place. The sunlight diffusion in the condensate layer can cause glare conditions and visual discomfort. In addition, window condensation is traditionally known to constitute a threat to the building envelope integrity, since it acts as a source for water accumulation that could be destructive to most organic-based and ferrous building components of the building envelope.

Seasonally, the hot, humid period of the year is also the longest, and atmospheric condensation on the external surfaces of windows becomes problematic to some air conditioned buildings. As a construction norm in hot, humid climates, single-glazed windows are used in most buildings whether or not they are air-conditioned. Insulated windows are neither popular nor economically attractive, since air temperature difference throughout the year, with the exception of summer, is relatively small. It has been demonstrated in literature that single glazed windows are often selected as a way to reduce capital costs [1]. Consequently, surface condensation potential is high on exterior surfaces of windows in air-conditioned buildings. In the presence of pollution, condensation can become a source for acid-related discoloration and deterioration of the exterior building surfaces. The severity of window surface condensation can range from a conspicuous film of condensation and aesthetic dissatisfaction, to serious deterioration of building materials and failure of building envelope performance. Condensation also encourages fungal growth on surfaces near windows that are exposed to the condensate run off. Moreover, there is an energy cost associated with condensation. Although the current window thermal assessment is limited to sensible heat gain or loss, it is reasonable as long as windows are insulated, hermetically sealed, small in area, or exposed to low relative humidity air compared to their surface temperatures. As larger windows are frequently used in buildings, window condensation becomes responsible for a small but sizable percentage of the total heat gain or loss associated with windows. This is particularly true for single-glazed windows and uninsulated double-glazed windows that are common in residential and light commercial buildings.

Proceedings of the Eighth Symposium on Improving Building Systems in Hot and Humid Climates, Dallas, TX, May 13-14, 1992

Previous studies [1, 2] have dealt with condensation problems under steady conditions, with emphasis on building surfaces and envelope components problems caused by condensation [2- 4]. Other studies have dealt with design guidelines for minimal condensation risk [5]. Daily and seasonal variations in air temperature, moisture content, and relative humidity add complexity to predictive models attempting to examine the condensation transient effect on thermal performance of windows. Moreover, when it comes to external surface condensation, no significant effort was found. As a matter of fact, condensation on or near external surfaces is not considered a problem [3]. This was based on the assumption that condensed water will eventually evaporate. This is true in cold, dry climates since the objective is to move the plane of interstitial condensation potential away from an insulation layer. However, in hot, humid climates, evaporation is difficult; thus, condensed water tends to remain for longer periods depending on the relative humidity level. The energy implication due to condensation has been investigated in the past. However, very little effort has been directed toward heat gain or loss associated with window surface condensation [6, 7]. The heat production due to the condensation process on internal window surfaces is discussed in [6].

In order to analyze the problem of external surface condensation and to estimate the heat gain associated with condensation, a model for estimating the mass condensation rate on the window's humid side and the energy loss associated with it is the subject of this paper. Unlike other studies, the work presented in earlier studies has demonstrated a serious attempt to consider the energy implications of window surface condensation through a more realistic modeling and simulation of atmospheric conditions [8-10]. The need for a condensation model that can account for the exact vapor-gas mixture of atmospheric air, can accommodate the fact that air is a non-condensable gas, and can recognize the gas component of atmospheric air dominates its gas-vapor mixture, is the focus of this study. A uni-dimensional transient finite-difference condensation procedure, based on a fully implicit formulation is developed and discussed in this paper. It accounts for condensation and the energy losses associated with it. Thermal analysis of both single- and insulated double-glazed windows under condensation conditions was modeled in this study. The external surface condensation process is analyzed, and a quantitative basis for predicting atmospheric water vapor mass condensation rate is developed. The theory of film condensation is utilized to establish a procedure by which mass condensation rate can be predicted for a mixture mainly consisting of non-condensable gases. Relations to determine interfacial temperature, T_{gi}, and the interfacial gas concentration, W_{gi}, for the atmospheric gas-vapor mixture which is dominated by non-condensable gases are given, along with the appropriate curves that were developed specifically to accommodate the conditions of the atmospheric air and to determine the interfacial temperature. In the following sections, the condensation process, its hygro-thermal analysis, the atmospheric air environment and the finite difference model are discussed along with results obtained from an experimental case study.

THE CONDENSATION PROCESS

Condensation occurs when water vapor comes in contact with a surface at a temperature below its saturation temperature. Excessive air-conditioning forces the temperatures of interior surfaces of walls and windows to drop. Unlike walls, low thermal resistance of windows makes their external surface temperature drop below the dew point temperature of the outdoor air. As a result, a continuous thin film of condensation that increases in thickness with time is formed on the glass exterior surface and then runs off the surface by gravitational forces causing deterioration to the building envelope.

Thermal analysis of windows has always been made in the absence of condensation and thus has never accounted for the latent component of heat gain or loss. Compared to other liquids, water has the greatest vaporization of latent heat. The release of latent heat of vaporization when atmospheric vapor changes its phase to liquid form, causes a rise in glass temperature. A sizable amount of latent heat is expected to be released as condensation of water vapor takes place. The released latent heat is an added building heat gain component in the case of external atmospheric condensation. It is an added heat loss component when internal surface condensation takes place. The increase in glass temperature due to summer condensation means additional heat gain to the air-conditioned indoor space. The magnitude of such heat gain depends upon the characteristics of the vapor and its temperature. The heat released is equal to the product of the latent heat of vaporization and the amount of the condensed liquid. The significance of condensation heat gain depends upon the atmospheric air temperature and relative humidity, indoor air temperature and the thermal characteristics of windows. As the relative humidity of the ambient air approaches saturation, the significance of window thermal resistance is greatly reduced since condensation, not limited to window surfaces, would probably spread to other exterior surfaces. Higher relative humidity is normally associated with still air conditions which further accelerates the condensation process.

HYGRO-THERMAL ANALYSIS

Temperature gradients across a window depend on many variables that are related to the thermal

properties of the window system, outdoor thermal conditions, and the indoor environment. Under steady-state conditions, the temperature gradient can be easily obtained in the absence of condensation. However, in the presence of condensation, the temperature gradient across a window is influenced by the latent heat component. In the presence of condensation, the pattern of the temperature gradient changes with time until the condensation process reaches the steady state and ultimately another temperature gradient is formed. Thus, the temperature gradient pattern is no longer linear, and can be described as unstable and transient until the steady-state condition is reached and a stable temperature gradient is formed. Therefore, the process of condensation should be considered transient. Since glass thickness is relatively small compared to the width and length of windows and since window frames are typically made out of wood or insulated metal, it is safe to assume a uni-dimensional heat transfer through window glazing in this study. To estimate heat gain or loss associated with window condensation, the time evolution of surface temperature profiles must be found.

The Critical Indoor Air Temperature, T_{ci}

The external surface temperature of a window glazing, T_{so}, can be expressed as:

$$T_{so} = T_o - \{ U_g \{ T_o - T_i \} / h_o \} \quad (1)$$

Where,

T_o = outdoor air temperature, °K

T_i = indoor air temperature, °K

h_o = external surface heat transfer coefficient, $W/m^2 \cdot K$

U_g = glazing overall heat transfer coefficient, $W/m^2 \cdot K$

If T_{dp} represents the dew point temperature of the outdoor air, the permissible lower limit of a given indoor air temperature below which external surface condensation occurs is defined as the critical indoor air temperature, T_{ci} and can be found from [8]:

$$T_{ci} = T_o \{ 1-(h_o / U) \} + \{ T_{dp} h_o / U \} \quad (2)$$

For the given values of T_o, h_o, and U_g, Eq.2 is graphically displayed so that a condensation region bounded by T_{ci} as a function of outdoor relative humidity, RH_o and indoor air temperature, T_i can easily be depicted. Two examples of the graphical representation given in [8] are shown in Fig.1 and Fig. 2 for two typical design wind conditions: still air and 3.4 m /s. It has been observed that the lesser the slope of T_{ci} due to wind speed, the larger the condensation region and the lower the indoor air temperature needed to form the condensation region. A simple comparison between still air and a typical value of 3.4 m/s for wind speed would show that the risk of condensation increases with decreased wind speed. Also, this indicates that buildings would be able to withstand cooler indoor air temperatures in summer without risking windows' external condensation during periods with higher wind speeds.

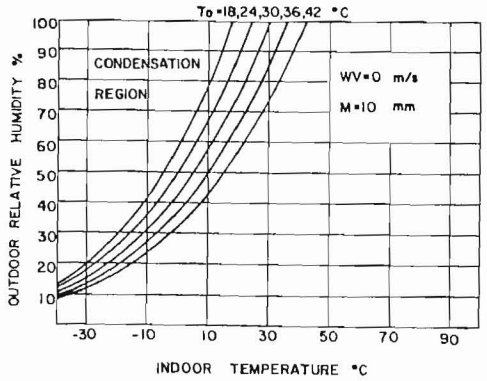

Fig. 1: Condensation region for a single glazed window at still air conditions

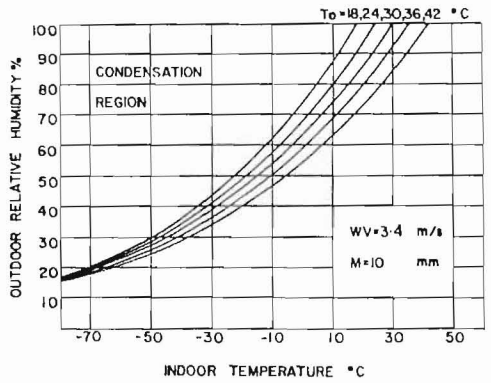

Fig. 2: Condensation region for a single glazed window at 3.4 m/s wind speed

Estimating the Mass Condensation Rate, M

There have been several theoretical and experimental studies on the prediction of mass condensation rate in the presence of a noncondensable gas [11-17]. The result of these studies cannot be used to predict mass condensation rate for situations where the gas-vapor mixture is dominated by a non-condensable gas such as air in the atmospheric air mixture. The presence of non-condensable gas, even in very small amounts, can have a significant effect on the mass condensation rate. The nature of the vapor is a useful criteria in classifying approaches to condensation analysis. According to the vapor classification given [18], a vapor is classified as either a single component vapor, a multi-component pure condensable vapor, a multi-component vapor with a non-condensable gas, or a

vapor with an immiscible liquid phase. A second form of classification is made with respect to the geometric shape of the condensation surface. This type of classification is based on the fact that surface geometry influences the hydrodynamics of condensate removal as well as the vapor-liquid interaction with respect to surface position. A third classification is according to the mode of condensation, being the direct contact mode, the homogeneous contact mode, the dropwise mode, or the film condensation mode [18]. For window condensation, the third classification seems most appropriate. Within this classification, the film condensation mode seems to be the most relevant and appropriate mode to describe surface condensation on windows as it occurs. Nusselt was the first to develop the analysis of film condensation. Filmwise condensation is a very common form of surface condensation. Nusselt's film condensation theory has the advantage over the commonly used mass transfer theory of being more accurate in describing the condensation process on vertical and other non-horizontal surfaces. The added accuracy is attributed to the ability of the film condensation theory to account for the effect of the water condensate film and the effect of the surface height. It is, however, limited to pure vapors. The main difficulty of applying Nusselt's film condensation analysis to window condensation problems is attributed to this limitation imposed by the fact that this theory assumes the presence of pure vapors. Atmospheric air is mostly gas and its water vapor is not a pure vapor. Nevertheless, it has been applied on window condensation problems in the past regardless of the great difference in the hygro-thermal behavior of atmospheric air and pure vapors. Fortunately, Nusselt's work has been extended by others to accommodate unique or special situations; those most relevant to the present study are given in [11, 12].

In film condensation analysis, the process of condensation occurs as the temperature of a surface becomes lower than the dew point temperature and vapor condenses forming a thin film on the surface. The film thickness increases with time and flows down a non-horizontal surface by gravitational forces. This process creates a film thickness gradient. Shown in Fig. 3. The latent heat is released at the vapor-liquid interface as a result of the vapor condensation process. The latent heat produced is then conducted through the condensate layer to the surface behind it. According to Nusselt's analysis of a pure vapor condensation, the average mass condensation rate of a pure vapor per unit width of a flat vertical surface with a constant temperature, T_s is given by [11]:

$$M = Q/h_{fg} = (4V_d / 3)\{C_p (T_{sat} - T_s) / h_{fg} Pr\}^{0.75} (gL / 4V_k)^{0.25} \quad (3)$$

where

M = average mass condensation rate per unit width, kg/m^{2}s
Q = heat released by condensation, W
T_s = constant average temperature of the surface, °K
T_{sat} = vapor saturation temperature, °K
L = surface height, m
V_d = dynamic viscosity, kg/m s
C_p = specific heat of liquid, J/kg °K
h_{fg} = latent heat of vaporization, J/kg
Pr = Prandtl number of liquid
g = gravitational constant, m/s
V_k = kinematic viscosity, m/s^2

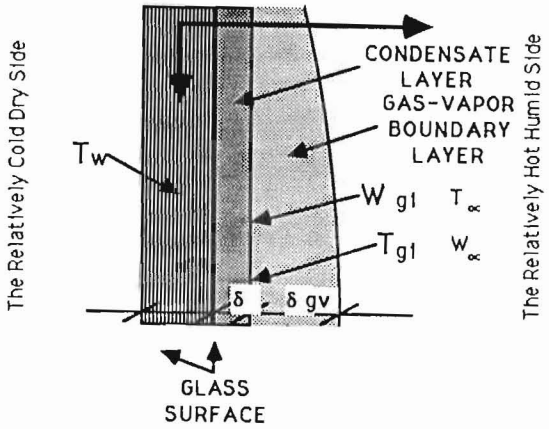

Fig.3: A schematic showing the condensation film thickness gradient

The Thermal Environment of Vapor Mixtures

The mechanism of heat transfer in the presence of a pure vapor differs from that in the presence of a vapor mixed with non-condensable gases. In the pure vapor case, one can safely assume perfect contact conditions between vapor and condensate liquid film. However, in the case on non-pure vapors, such contact is no longer perfect due to the presence of non-condensable gases. As a vapor containing non-condensable gases condenses, the non-condensable gas is left at the surface, forming a gas layer near the surface that would act as a resistance layer to the next cycle of condensation. This means an added resistance to vapor attempting to diffuse through the gas-layer to reach the cold surface to condense [18]. In atmospheric conditions, vapor has to diffuse through the non-condensable gases before it comes in contact with the cold surface inducing condensation. This implies an added resistance to heat flow towards the condensing surface which is caused by the presence of non-condensable gases. The added resistance to vapor diffusion causes a drop in the partial pressure of the condensing vapor which in turn causes the temperature of the outer surface of the condensate to drop below saturation temperature.

The Nusselt's film condensation approach is adjusted to account for the difference between pure vapor and vapor in a vapor-gas mixture with emphasis on vapor in the atmospheric air which is a vapor-gas mixture dominated by non-condensable gases. Condensation analysis for a vapor mixture containing a non-condensable gas has been attempted before [11-17]. The diagrammatic representation shown in Fig. 3 illustrates a condensate layer of a thickness "d" bounded by the cold surface from one side and the gas-vapor layer on the other side. The determination of the temperature of the condensate outer surface, the interfacial temperature, T_{gi}, and the interfacial gas concentration, W_{gi}, are fundamental requirements for any realistic assessment of condensation. However, it is a complicated process since it requires simultaneous solutions of heat transfer, mass and momentum equations in both the liquid and the vapor-gas mixture. A typical routine to determine the interfacial temperature, T_{gi}, and the interfacial gas concentration, W_{gi}, at the interface between the condensate layer and the gas-vapor boundary layer is described [11] and is based upon momentum and energy equations for the condensate layer. Nusselt's theory has been tested under conditions closely satisfying his assumption and has been generally confirmed [19]. This routine provides a set of curves that are useful in predicting the heat transfer when the vapor contains a small percentage of a non-condensable gas ($\leq 3\%$). In situations with non-condensable gas domination in the vapor-gas mixture, such as in the atmospheric air (i.e $\leq 90\%$), there is no similar estimation routine. Consequently, a major objective of this study is to adjust the film condensation theory to be applicable to the non-condensable atmospheric gas-vapor mixtures. The approximate solution [13] to substitute the complex differential equations needed for the exact solution has never been popular in most gas-vapor mixtures, since its accuracy decreases significantly as the non-condensable gas percentage decreases. Fortunately, the conditions of the atmospheric air have made the use of such an approximate solution very attractive since it produces a solution almost identical to the exact solution at atmospheric conditions (non-condensable gases % is $\leq 90\%$). The curves developed for these high percentages of non-condensable gases using the approximate solution are shown in Fig. 4 and Fig. 5. The concentration range is between 0.94 and 0.99 ($94\% \leq$ non-condensable gas $\% \leq 99\%$).

Evaluating Interfacial Temperature, T_{gi}

The evaluation of T_{gi} is made through a trial and error approach. Knowing the surface temperature, T_{so}, one can first assume a value of T_{gi} and then evaluate the interfacial gas concentration, W_{gi}, using the appropriate curve from Figs. 4 and 5. The next step is to use the value obtained for W_{gi} to evaluate the corresponding interfacial vapor pressure, P_{vi} as follows:

$$P_{vi} = \{ (1-W_{gi}) / (1- (1- (m_v / m_g)) W_{gi)} \} P_{tot} \quad (4)$$

where,

P_{tot} = total pressure, N/m^2
m_v = vapor molecular weight, kg /Kmol
m_g = gas molecular weight, kg/Kmol

The corresponding saturation pressure, P_{sat}, to this interfacial vapor pressure is calculated or obtained from vapor tables. When T_{gi} is assumed equal to the saturation pressure Tsat, T_{gi} can then be used to calculate the mass condensation rate. If results are found incompatible, the process is repeated with a more appropriate value for T_{gi}.

In the presence of a non-condensable gas, the mass condensation rate for the same condition is always less than that predicted by Eq. 3. This can be confirmed by the fact that non-condensable gas remains on the surface during the condensation process. As a result, condensation can continue only if the vapor diffuses through the gas-vapor mixture before it reaches a relatively cold surface. This added resistance to vapor diffusion causes a drop in the partial vapor pressure, which in turn causes the temperature of the outer surface to drop below the saturation temperature, T_{sat}. In order to utilize Eq.3 in the presence of non-condensable gas, T_{sat} needs to be replaced by an interfacial temperature T_{gi}. However, the analysis needed to evaluate T_{gi} involves simultaneous solution of heat, mass and momentum transfer equations for the liquid and vapor gas mixture. Sparrow and Lin [11] provided a solution in the form of a set of figures where two families of curves represent the interfacial gas concentration, W_{gi}, and the interfacial vapor pressure, P_{vi}. By using the appropriate figure, one can determine the interfacial temperature by trial and error and then substitute it for T_{sat} in Eq. 3. Although this solution is for non-condensable gases, it can only be used if the non-condensable gas component is very small (3%). In atmospheric air mixtures, the non-condensable gas constitutes the majority of the mixture (97%). Therefore, a similar set of curves, suitable for atmospheric conditions, was developed for predicting mass condensation rate, M, for gas-vapor mixtures dominated by a non-condensable gas. The complex solution process has almost made it difficult. The approximate solution available [13] is to our advantage since its accuracy increases as the non-condensable gas component increases. It is able to provide an identical solution to the exact solution at 97% non-condensable gas domination which best fits atmospheric conditions. This approximate solution is in the form of a simple algebraic equation relating heat and mass transfer parameters to the fluid/gas properties. As shown in Fig. 4 and Fig. 5, two families of curves were

generated by utilizing this approximate solution. The generated curves are for gas concentration ranges from 0.94 to 0.99. Now, the interfacial temperature can be obtained by trial and error and then used to replace T_{sat} in the mass condensation equation to determine the mass condensation rate M according to Eq. 3.

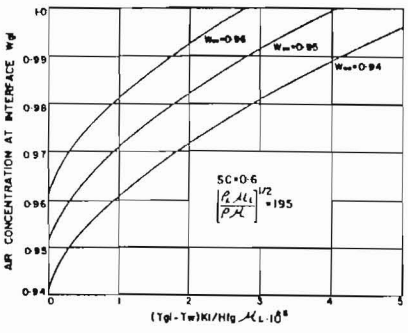

Fig. 4: Air Concentration at the interface for the atmospheric conditions with W_{∞}=94 to 96

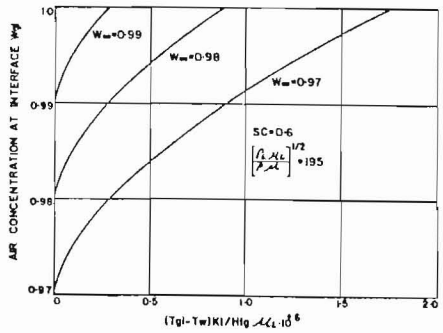

Fig. 5: Air Concentration at the interface for the atmospheric conditions with W_{∞}=97 to 99

THE FINITE-DIFFERENCE MODEL

The condensation process is transient in nature and the thickness of a window is generally very small as compared to the width or length. Thus, the model is based on transient and uni-dimensional analysis. The transient, uni-dimensional partial differential equation of heat conduction was approximated through the use of a fully implicit formulation of the finite-difference method to form a set of algebraic equations. Each is expressing the temperature of a given thermal node as a function of temperatures of the other surrounding nodes within the window region in question. The fully implicit scheme was chosen to ensure stability of the solution and its accuracy without imposing unnecessary restrictions over the size of the time step. In the analysis of surface condensation, several assumption were made. During the time at which condensation occurs, temperature, humidity and surface heat transfer coefficients were assumed to be constant. On the condensing side, the reference temperature at which condensation occurs is assumed to be the immediate surface temperature before condensation. The thermal resistance of the condensate film has a negligible effect on the conductive heat transfer due to the temperature differential across the window.

A choice had to be made between explicit and implicit formulations of this technique. Although the explicit formulation offers a simpler path, it has a restriction on the maximum size of the time step to ensure solution stability. On the other hand, since implicit formulation is relatively complex due to the simultaneous solution requirements for all nodal temperatures at each time step, this formulation is able to provide a stable solution independent of the size of time step selected. However, its accuracy was found to improve with smaller time steps [20]. The most accurate and efficient implicit scheme that is commonly used is that of Crank and Nicolson [18]. The accuracy of this scheme is based on the use of arithmetic mean values of the derivatives at the beginning and at the end of all time intervals [21]. Near a closed-form solution, the time step is very small. Thus, by reducing the time step, accuracy of this scheme increases. Also, it should be noted that oscillation due to large time steps would result in inaccurate solution. The fully implicit scheme of the finite difference has an advantage over the implicit formulation when large time steps are required. Thermal analysis of buildings deals with materials, thicknesses and thermal conditions that typically would require large time steps ranging from a minute to an hour. Thermo-physical properties of various building materials are available in most standard heat transfer books [19-24].

The fully implicit scheme was employed in order to achieve desired accuracy that is independent of the size of the time step. For the purpose of simplification and application of the finite-difference analysis to condensation heat transfer of windows, the following assumptions were made:

i) During condensation, air temperature and relative humidity on both sides of the window remain constant;

ii) Window's surface heat transfer coefficients are constant;

iii) Surface temperature immediately before condensation occurs is considered the temperature at which condensation starts;

iv) Window is infinite in width and length;

v) Window absorption to solar heat gain is neglected; and

vi) Thermal resistance of the condensate film has no effect on the heat transfer due to temperature difference.

Based on the above assumptions and using the first law of thermodynamics, the differential formulation of a uni-dimensional transient heat conduction can be expressed as [23]:

$$dq_x = dq_{x+\Delta x} + (\partial E / \partial t) \quad (5)$$

and by utilizing the definition of the partial derivative, Eq. 5 becomes:

$$dq_x = dq_x + \partial (dq_x / \partial x)\, dx + (\partial E / \partial t) \quad (6)$$

and by introducing the Fourier Law of Conduction, Eq. 6 becomes:

$$(\partial/\partial t)(\rho C_v T) = (\partial/\partial x)(k (\partial T/\partial x)) \quad (7)$$

where,

E = Energy, Joule
ρ = density, kg/m^3
C_v = specific heat, j kg/°K
T = temperature, °K
k = thermal conductivity, m^2/s

In order to utilize the finite-difference method, the window thickness is subdivided into imaginary layers, each is represented by a thermal node. These nodes, classified as interior and exterior nodes, are spaced equally by a distance dx as shown in Fig, 6.

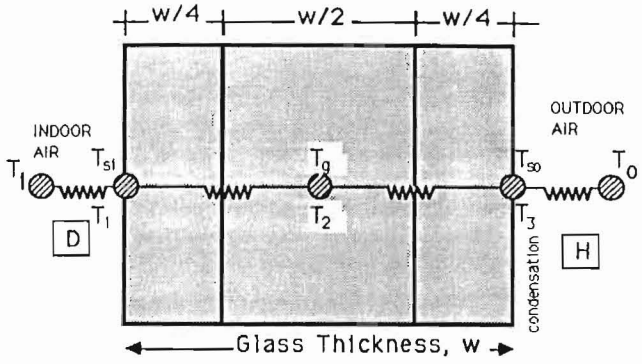

Fig. 6 : Thermal network of a single glazed window

The energy balance of an interior node is then expressed as:

$$(-k/\Delta x)(T_m - T_{m-1}) = -k(T_{m+1} - T_m) + \rho \Delta x^2 C_v ((T_m - T_m)/\Delta t) \quad (8)$$

Where T is the present temperature, **T** (bold) is the future temperature after a time step Δt and subscripts m denote node number m, $m-1$ the node immediately before it, and $m+1$ the node immediately after it. In a similar manner, one can express the energy balance of an exterior node as:

$$(-k/\Delta x)(T_{m+1} - T_m) = q_s + 0.5 \rho \Delta x C_v (T_m - T_m)/\Delta t \quad (9)$$

where T_m is the future temperature at node m at time $t+\Delta t$ and q_s is the total heat transfer to or from a unit area. The single glazed window is assumed to consist of three layers, each one is thermally represented by a thermal node. The three nodes of the three layers of a single-pane window are shown in Fig.6. The first is a surface node facing the dry side. The second is a core node representing the core of the glazing. The third is a surface node facing the humid side. In such a generalization, one can conduct condensation analysis independent of the actual position of the surface at which condensation occurs. Denoting the humid side by subscript H and the dry side by subscript D, it is possible to express the energy balance of the three nodes for both types of condensation using the same set of equations which is also able to accommodate variable or constant conditions on both sides of the window. In hot, humid climates, the humid side faces the outside while in a cold climate, the humid side faces the inside. Since there are two possible sides for window surface condensation, the model is made to handle both internal and external surface condensation. Three nodes can be identified for the single glazed window shown in Fig. 6. The first node is the surface node facing the dry side, the second is the the core node within the glass itself, and the third is a surface node facing the humid side. The set of algebraic equations for the single glazed case is written as follows:

for node 1 on the dry side, the energy balance is expressed as:

$$T_1 = (1 + 2P_1 + 2P_2)\, T_1 - 2P_1 T_2 - 2 P_2 T_D \quad (10)$$

for node 2 representing the core layer,

$$T_2 = (1 + 2P_1)\, T_2 - P_1 T_1 - P_1 T_3 \quad (11)$$

and for node 3 on the humid side,

$$T_3 = (1+2P_1 + 2P_3)\, T_3 - 2P_1 T_2 - 2P_3 T_H - P_4 M \quad (12)$$

where T_D and T_H are the air temperatures on the dry and humid sides respectively. M is the mass condensation rate per unit area. The parameters P_1, P_2, P_3, and P_4 are defined as:

$$P_1 = k_g \Delta t / F,$$

$$P_2 = \Delta t\, h_D / F,$$

$P_3 = \Delta t\, h_H / F$, and

$P_4 = 2\, \Delta t\, h_{fg} / F$ (13)

k_g is the glass thermal conductivity, h_D and h_H are the surface heat transfer coefficients on the dry and humid sides respectively , h_{fg} is the latent heat of vaporization in J /kg and F is the product of glass density ρ_g, glass specific heat, C_v, and the nodal spacing Δx. The input data can be constant only when constant conditions are simulated. Otherwise, their values are those of the next time step.

The modeling of a double-glazed window is a straightforward extension of the single- glazed window model. The only difference is to account for the presence of an inter-pane air-gap. For simplification and convenience, the air gap thickness shown in Fig. 7 is taken as twice the glass thickness which is typical practice for most double-glazed windows.

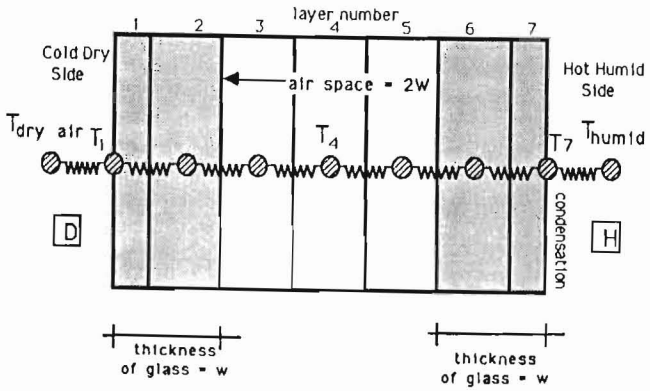

Fig. 7 : Thermal network of a double-glazed window

The heat transfer across the air-gap is assumed to be by conduction only. Radiative heat exchange through the air-gap is accommodated by an equivalent increase of the actual conductivity of the air. Thus, conductive equivalence of the radiative heat transfer within the air-gap is considered constant. The conductive equivalent to radiative heat transfer is taken as 0.054 W/m K. A value of 3.3 W/m^2K is used for h_r when a glass emittance of 0.82 was used. For a 9 mm air space, the heat transfer coefficient, h_r, is about 3 W/m^2K. In order to maintain a simple equidistant scheme for the spacing between thermal nodes, each pane is divided into two layers and the air gap is divided into three layers as shown in Fig. 7. The energy balance of a double-glazed window can now be described by the following seven equations:

for node 1 on the dry side,

$$T_1 = (1+2P_1 + 2P_2)\, T_1 - 2P_1\, T_2 - 2P_2\, T_D \quad (14)$$

for node 2 through node 6,

$$T_2 = (1+P_1 + P_5)\, T_2 - P_1\, T_1 - P_5\, T_3 \quad (15)$$

$$T_3 = (1 + P_6 + P_7)\, T_3 - P_6\, T_2 - P_7\, T_4 \quad (16)$$

$$T_4 = (1+ 2P_7)\, T_4 - P_7\, T_3 - P_7\, T_5 \quad (17)$$

$$T_5 = (1 + P_6 + P_7)\, T_5 - P_7\, T_4 - P_6\, T_6 \quad (18)$$

$$T_6 = (1+ P_1+P_5)\, T_6 - P_5\, T_5 - P_1\, T_7 \quad (19)$$

and for node 7 on the humid side,

$$T_7 = (1+2P_1 + 2P_3)\, T_7 - 2P_1\, T_6 - 2\, P_3\, T_H - P_4\, M \quad (20)$$

where P_5, P_6, and P_7 are:

$P_5 = P_1\, k_{ca} / k_g$,

$P_6 = P_5\, Cp_g / Cp_a$, and

$P_7 = P_1\, k_a\, Cp_g / K_g\, C_{pa}$ (21)

where P_a and Cp_a are the density and specific heat of air respectively. k_{ca} is the combined air-glass thermal conductivity calculated as $\{k_{ca}= (2\, k_a\, k_g)/ (k_a+k_g)\}$

It should be noted that the time required for the internal surface temperature to rise as a result of the released latent heat is problem dependent. Fig.8 shows the variation of the internal surface temperature with time for two common limits of indoor air temperature. It can be seen that temperature rise due to condensation is almost doubled when indoor air temperature is reduced from 24 °C to 18°C. Fig. 8 shows that internal surface temperature increases as outdoor relative humidity is increased. The significance in the rise in internal surface temperature stems from the fact that condensation represents an added component of window heat gain. The rate of heat gain due to condensation is small compared to conduction or transmission gains, yet is significant when the total area of the windows constitutes the majority of the external wall area. Condensation heat gain is illustrated in Fig. 9 as a function of the atmospheric relative humidity and air temperature. As an example, for T_i =21° , T_o = 35° , and RH_o = 90%, the heat gain rate due to condensation was found to be about 10 W / m^2 for a single-glazed window.

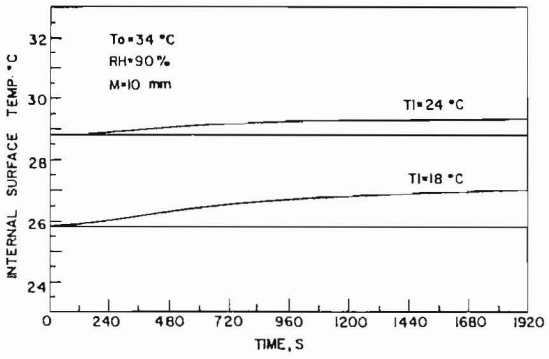

Fig. 8: Variation of internal surface temperature with time under two common indoor air temperature settings

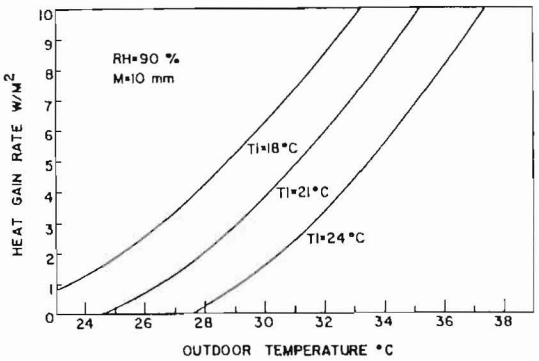

Fig. 9: Heat gain rate due to external condensation for 10 mm thick single glazed window with outdoor relative humidity of 90%

For both single and double windows, the mass condensation rate, M, must be calculated at the beginning of each time interval in order to solve simultaneously for nodal temperatures of the corresponding set of equations. The tri-diagonal matrix iteration technique is used for the simultaneous solution for all nodal temperatures. In order to validate the model, an experimental study was carried out where more than 50 tests were conducted. The experimental set-up used in testing a 5 mm single glazed window is shown in Fig. 10. The set up is described simply as a hot box with humidification capability from a steam generator. The window is inserted between a cold box and a hot box. Temperatures were measured for the glass surface as well as in five locations within the box air. Their average was used to represent the air temperature within the box. The deviation of any single temperature measurement from the average never exceeded 1°C. All measurements were logged to a data acquisition system with the exception of the

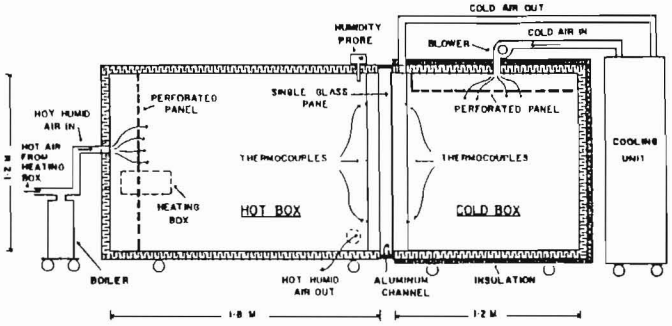

Fig. 10: Schematic showing cross-sectional view of test set-up

measuring of the amount of the collected condensate during each experiment. Eighteen tests were specifically compared to model results. On average, mass condensation rates that are based on the measurement data were found to be about 16% lower than calculated values. This discrepancy, was to some extent, expected due to oversimplifyed testing using inexpensive experimental set-up, where maintaining simultaneously both humidity and temperature at constant levels was a difficult task. Nevertheless, the experimental results are consistent with model output, even though the tests were conducted at different hygro-thermal conditions. In previous studies, there is evidence that measured heat transfer coefficients were about 20% higher than Nusselt's theory suggest [18]. This could also indicate that the present results are in agreement with those measured values given by [18]. The test conditions and results are summarized by Figs. 11 through 16.

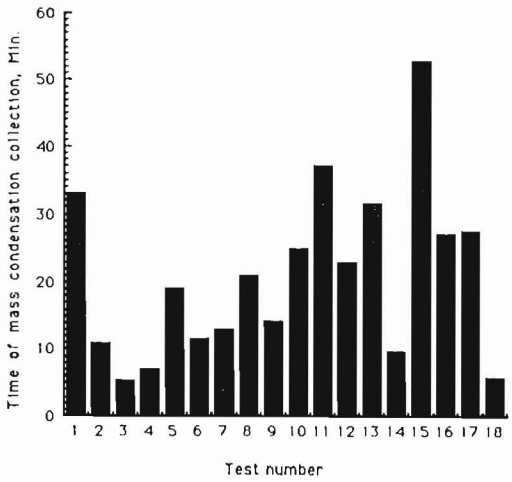

Fig. 11: Mass Condensation Period

As shown in Figs. 11, 12, and 13, the condensation period, the humidity and temperature conditions along with glass temperature in these tests are shown. Total amount of mass condensation obtained during each test is shown in Fig. 14.

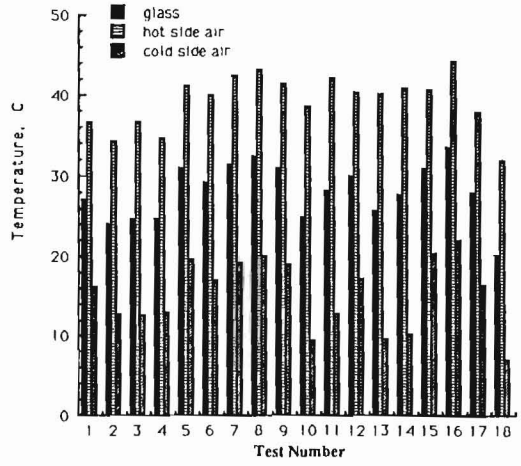

Fig. 12: Measured temperatures of glass surface, hot side air, cold side air for 18 different tests

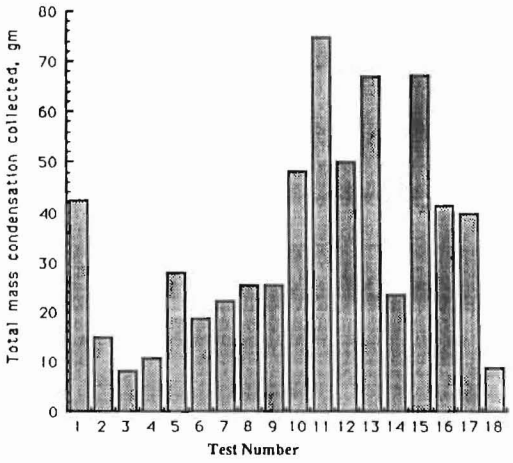

Fig. 14:Total mass condensation collected during each test period

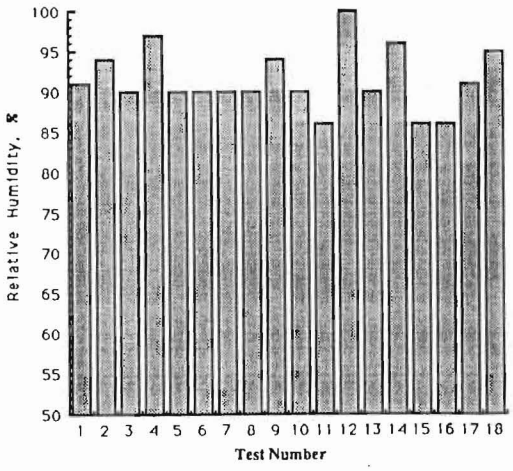

Fig. 13: Humidity levels in each test

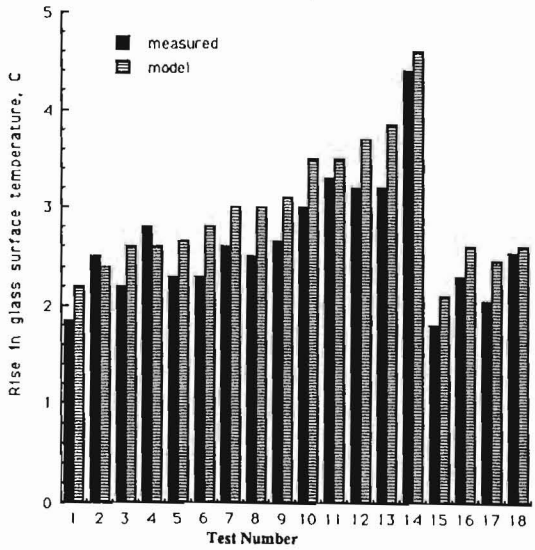

Fig. 15: Calculated versus measured rise in glass surface temperature for each test

Comparison between the model and measurements with respect to the rise in the window surface temperature and the mass condensation rate are shown in Figs. 15 and 16. The experimental procedure for measuring the mass condensation rate was conducted as a means for the verification of the proposed concept. As shown in Fig. 15 and 16, a comparison between calculated values of temperature rise and mass condensation rate and values obtained from measurements were made and good agreements were found.

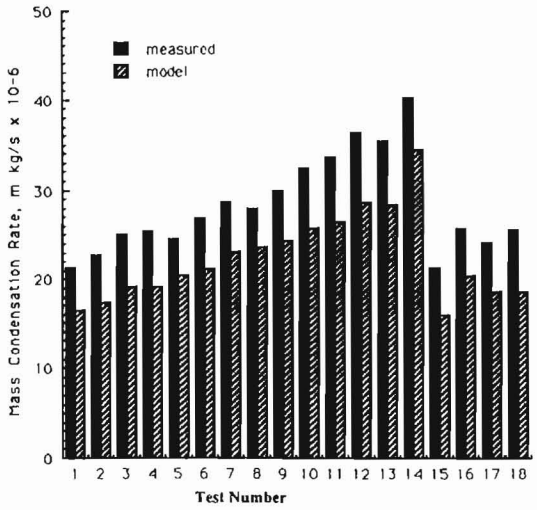

Fig. 16: Condensation region for a single glazed window at still air conditions

CONCLUSION

This study has provided an insight into atmospheric condensation problems in general, and exterior condensation in hot, humid climates in particular. The external surface condensation of windows has been analyzed with respect to the condensation potential and the identification of the condensation region. The mass condensation rate has been evaluated for the atmospheric air mixture that is dominated by a non-condensable gas using a new approach. This approach extends the use of the film condensation theory for pure vapors to estimate the mass condensation rate for gas-vapor mixtures dominated by non-condensable gas such as the atmospheric air. Moreover, heat gain due to external surface condensation cannot be directly evaluated by the current procedures employing mass transfer due to vapor pressure difference, such as the Davies model [6], in which glass thermal resistance is neglected, and consequently the temperature across window thickness is considered uniform. The present study is based on evaluating the condensation film interfacial temperature, then determining the mass condensation rate as well as the heat transfer rate. The interfacial temperature needed for estimating the mass condensation rate on the window's surface has been graphically presented for atmospheric gas-vapor mixture assuming constant surface temperature with window condensation. The benefits from the present study are not limited only to the prediction of the mass condensation rate using film condensation analysis, but are also useful in accommodating the time dependency nature of window condensation analysis, and the consequent potential of improved assessment of net heat gain or loss through windows.

The proposed procedure will enable designers to determine the magnitude of the temperature gradient across the thickness of single- and double-glazed windows, the effect of variable indoor and outdoor conditions on surface temperature and the condensation starting point, the magnitude of surface temperature variation during the condensation process, the mass condensation rate as a function of the interfacial temperature and the resulting heat gain or loss associated with window condensation.

The energy loss implication of window condensation was found to be reasonably small when compared to other window losses. However, when the total window surface area of a building is significant, latent energy losses due to condensation should be considered. The proposed model has the ability of assessing window heat gain or loss in the presence of condensation. Heat loss associated with condensation can amount to about one-fifth the total heat loss of a single-glazed window.

Results from tests agreed reasonably with the proposed model. It can also be used in estimating heat gain or loss associated with condensation. A specifically constructed experimental set-up has been utilized to verify this model. More experimental verification would be very valuable. Further work is essential to extend the model to accommodate situations where constant surface temperature cannot be assumed. In other words, the effect of the small rise in surface temperature on the time-dependent mass condensation rate can be considered. In short, the proposed procedure makes it possible to assess window energy performance and thermal loads associated with external window condensation in hot humid climates and internal condensation in cold climates.

ACKNOWLEDGEMENT

The authors are grateful to the Natural Sciences and Engineering Research Council of Canada for the financial support and encouragement.

REFERENCES

1. Wilson, A.G., 1973, " Condensation on Inside Window Surfaces," Canadian Building Digest, vol. 137, no. 2, pp 4.1-4.4.
2. Dutt, G.S., 1979, " Condensation in Attics: Are Vapour Barriers Really the answer ?,", Energy and Buildings, vol. 1, pp 251-258.
3. Oxley, T.A., Gobert, E.G., 1983, Dampness in Buildings, Page Bros Ltd., Norwich, Norfolk,
4. Decker, R., 1984, " Condensation and Mould Growth in Dwellings- Parametric and Field Study," Building and Environment, vol. 19, no. 4, pp 243-250.
5. Achenbach, P.R., Terchsel, H.R., 1982, " Evaluation of Current Guidelines of Good Practice for Condensation Control In Insulated Building

Envelopes," ASHRAE/DOE Conference, Las Vegas, Nevada, pp 1090-1107.
6. Davies, M.G., 1973, " Computing the Rate of Superfacial and Interstitial Condensation," Building Science, vol. 8, no.2, pp 97-104.
7. Davies, M.G., 1977, " The Environmental Temperature Procedure and Moisture Movement in an Enclosure, " Building Services Engineer, vol. 45, no. 6, pp 83-92.
8. El Diasty, R., Budaiwi, I, 1989, " External Condensation on Windows," Construction and Building Materials, vol. 3, no. 3, pp 135 -139 .
9. El Diasty, R., Budaiwi, I., 1989, " Prediction of Mass Condensation Rate for Gas-Vapour Mixture Dominated by a Non-Condensable Gas," 12th Canadian Congress of Applied Mechanics, vol.2, pp 734 -735 ,Ottawa, Ontario, Canada.
10. El Diasty, R., Budaiwi, I., 1989, " Window External Surface Condensation in Hot Humid Climates," 11th Intl. Congress, CIB'89: Quality for Building Users Throughout the World, vol. 1, pp 274-283, Paris, France.
11. Sparrow, E.M., Lin, S.H., 1964, " Condensation Heat Transfer in the Presence of a Noncondensable Gas," Journal of Heat Transfer, Vol. 86, pp 430-438.
12. Minkowycz, W.J., Sparrow, E.M., 1966," Condensation Heat Transfer in The Presence of Noncondensable Interfacial Resistance, Super Heating, Variable Properties and Diffusions," Intl. Journal of Heat and Mass Transfer, Vol. 9, pp 1125-1144.
13. Rose, J.W., " Condensation of a Vapour in the Presence of a Noncondensing Gas," Intl. Journal of Heat and Mass Transfer, Vol. 12, pp 233-237, 1969.
14. Denny, V.E., Jusionis, V.J., 1972, " Effect of Noncondensable Gas and Forced Flow on Laminar Film Condensation," Int. J. of Heat and Mass Transfer, vol. 15, pp 315-326.
15. Felicione, F.S., Seban, R.A., 1973, " Laminar Film Condensation of a Vapour Containing a Soluble Noncondensable Gas," Int. J. of Heat and Mass Transfer, vol. 16, pp 1601-1610.
16. Al-Diwany, H.K., Rose, J. W., 1973, " Free Convection Film Condensation of Steam in the Presence of Non-Condensing Gases", Int. J. of Heat and Mass Transfer, vol. 16, pp 1359-1369.
17. Mori, Y., Hijikatta, K.J., 1973, " Free Convection Condensation Heat Transfer with Noncondensable Gas on a Vertical Surface," Int. J. of Heat and Mass Transfer, vol. 16, pp 2229-2240.
18. Bell, K.J., Panchal, C.B., 1978, " Condensation," Proceedings of the 6th Intl.Heat Transfer Conference, Toronto, Canada, vol. 6, pp 361-375.
19. Thomas, L.C., 1980, Fundamentals of Heat Transfer, Prentice-Hall, New Jersey.
20. Croft, D.R., Lilley, D.G., 1977, Heat Transfer Calculation Using Finite Difference Equations, Applied Science Publisher, London, UK.
21. Myers, G.E., 1965, Analytical Methods in Conduction Heat Transfer, Prentice Hall, N.J.
20. Ozisik, M.N., 1985, Heat Transfer, A Basic Approach, Mcgraw-Hill, New York.
21. Holman, J.P., 1981, Heat Transfer, McGraw-Hill , 5th edition, N.Y.
22. ASHRAE Handbook of Fundamental, 1989, ASHRAE Inc., N.Y.